

# Numerical Study on Bouncing and Separation Collision Between Two Droplets Considering the Collision-Induced Breakup

Gwon Hyun Ko<sup>b</sup>, Hong Sun Ryou<sup>a,\*</sup>, Nahm Keon Hur<sup>c</sup>,  
Seung Woo Ko<sup>d</sup>, Myoung O Youn<sup>e</sup>

<sup>a</sup>*Institute of Advanced Machinery and Design, Seoul National University, San 56-1, Shillim-Dong, Gwanak-Gu, Seoul, 151-744, Korea*

<sup>b</sup>*Corresponding Author, School of Mechanical Engineering, Chung-Ang University, Heukseok-Dong, Dongjak-Gu, Seoul, 156-756, Korea*

<sup>c</sup>*Department of Mechanical Engineering, Sogang University, 1 Sinsoo-Dong, Mapo-Gu, Seoul, 121-742, Korea*

<sup>d</sup>*Department of Mechanical Engineering, Chung-Ang University, Heukseok-Dong, Dongjak-Gu, Seoul, 156-756, Korea*

<sup>e</sup>*Department of Architecture, University of Seoul, Jeon Nong-Dong, Dong Daemoon Gu, Seoul, 130-743, Korea*

(Manuscript Received June 29, 2006; Revised December 1, 2006; Accepted January 18, 2007)

---

## Abstract

The main purpose of the present study is to perform numerical study on bouncing and separation collision between two droplets considering the collision-induced breakup. In this study, the collision model proposed in our previous study is used for simulation of collision-induced breakup, and we modify this model to consider the effect of liquid property on the behavior of droplet-droplet collision. This collision model is based on the conservation laws for mass, momentum, and energy between before and after collision and provides several formulae for post-collision characteristics of colliding droplets and satellite droplets. Improving the accuracy of the model, in this study, appreciate criterion for bouncing collision is added and dissipation energy during collision process is newly modeled. To validate the new model, numerical calculations are performed and their results are compared with experimental data published earlier for binary collisions of water, propanol, and tetradecane droplets. It is found from the results that the new model shows good agreement with experimental data for the number of satellite droplets. It can be also shown that the predicted mean diameter by the new model decrease with increasing the Weber number because of the collision-induced breakup, whereas the O'Rourke model fails to predict the size reduction via the binary droplet collision.

*Keywords:* Collision; Break up; Bouncing; Separation

---

## 1. Introduction

Collision dynamics of liquid droplets is important in evolution of sprays used in various industrial applications. In dense spray system and inter-spray impingement system (O'Rourke, 1981; Arai and Saito, 1999), droplet collision can significantly affect the spray characteristics, such as drop size and velocity

distribution. The outcomes from binary droplet collision are classified four different types: bounce, coalescence, reflexive separation, and stretching separation, as seen in Fig. 1. Many researchers (Ashgriz and Poo, 1990; Qian and Law, 1997; Brenn et al., 2001) observed that the separations produce the satellite droplets from the interacting parts between two colliding droplets, and in turn results in the size reduction in droplets see Fig. 2(c) & 2(d). This procedure is called a collision-induced breakup process whose effects are more pronounced as Weber

---

\*Corresponding author. Tel.: +82 2 820 5280; Fax.: +82 2 813 3669  
E-mail address: cfdmcc@cau.ac.kr

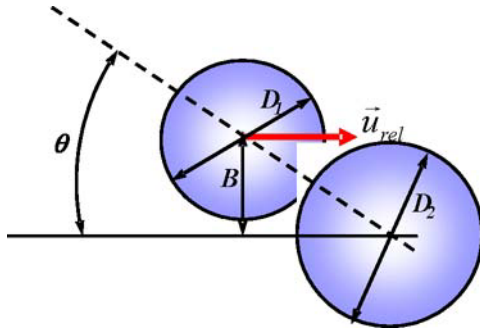


Fig. 1. Kinetic and geometric parameters of the droplet collision.

number increases. In addition, it is well known that the droplet collision phenomena highly rely upon the droplet property. By contrast with the collision of water droplets, the bouncing phenomena occur over the wide range of Weber number, and also the surface tension energy loss becomes more significant in the collision of hydrocarbon fuel droplets.

In most of numerical simulation on spray dynamics, the model of O'Rourke (1981) has been commonly used for the droplet collision process. However, there are some problems that the O'Rourke model includes only coalescence and grazing separation. It means that the O'Rourke model cannot mimic other important processes related to the binary collision, e.g., reflexive and stretching separations, and corresponding formation of satellite droplets. Moreover, because the O'Rourke model was derived on the basis of binary collision of water droplets, it may not be suitable for calculation of collision processes of fuel droplets. Recently, we (Ko and Ryou, 2005a, 2005b) proposed the new droplet collision model considering droplet collision-induced breakup process with the formation of satellite droplets. This model consists of several equations to determine the post-collision characteristics of colliding droplets and satellite droplets. These equations were derived from the conservations of droplet mass, momentum, and energy between before and after collision, and made it possible to predict the number of satellite droplets, and the droplet size and velocity in the analytical way. In this model, however, the liquid property effects including bouncing phenomena and surface tension energy loss of fuel droplets are hardly considered.

The main purposes of the present study are thus to perform numerical study on the binary droplet collision considering the collision-induced breakup and the effects of liquid property. The collision model proposed in our previous study (Ko and Ryou, 2005a,

2005b) is used for simulation of collision-induced breakup, and this model is modified to consider the effect of liquid property on the behavior of droplet-droplet collision. The comparisons of numerical predictions with experimental data (Ashgriz and Poo, 1990; Qian and Law, 1997) are conducted for post-characteristics of binary droplet collision process.

## 2. Droplet collision model

### 2.1 Binary droplet collision phenomena

Generally, the droplet collision process is described by three non-dimensional parameters as follows (Ashgriz and Poo, 1990, Qian and Law, 1997, Brenn et al., 2001);

$$We = \rho D_1 |\vec{u}_{rel}|^2 / \sigma \quad (1)$$

$$\Delta = D_1 / D_2, \quad (2)$$

$$b = 2B / (D_1 + D_2), \quad (3)$$

where  $We$  is the Weber number based on droplet diameter,  $\Delta$  the droplet size ratio, and  $b$  is the impact parameter.  $\rho$  and  $\sigma$  are the density and the surface tension of liquid phase, and the subscripts 1 and 2 represent smaller and larger droplets, respectively.  $B$  is calculated by taking the distance from the center of one droplet to the relative velocity vector,  $\vec{u}_{rel}$ , placed on the center of the other droplets, as illustrated in Fig. 1. The outcomes from collision are classified four different types: bounce, coalescence, reflexive separation, and stretching separation, as seen in Fig. 2. As two droplets impinge each other, the gas between them is trapped and the pressure increases inside this gap. If relative velocity of droplets is not enough to overcome the pressure force, two droplets do not impinge and go away from each other. This is referred to as bouncing. For higher relative velocity, on the other hand, one droplet contacts another directly and in turn coalescence process takes place between them. At high Weber numbers, the droplets have excess kinetic energy, which leads to the separation of droplets from droplet coalesced tentatively. The temporarily coalesced droplets tend to undergo a reflexive separation and a stretching separation at low and high impact parameters, respectively. Many researchers (Ashgriz and Poo, 1990, Qian and Law, 1997, Brenn et al., 2001) observed that the separations produce the satellite droplets from the interacting parts between two colliding droplets, and in turn

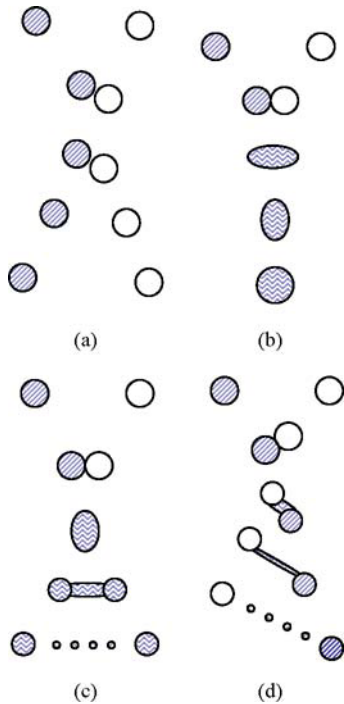


Fig. 2. Diagram of collision regimes: (a) bouncing; (b) coalescence; (c) reflexive separation; (d) stretching separation.

results in the size reduction in droplets. This procedure is called a collision-induced breakup process whose effects are more pronounced as Weber number increases.

**2.2 O'Rourke model**

Among outcomes of droplet collision, the O'Rourke (1981) model considers two regimes of permanent coalescence and separation, but ignores the formation of the satellite droplets. Figure 3 shows the boundaries between the regimes adopted in the O'Rourke model for the collision of equal-sized droplets. Followings explain the relationships in O'Rourke model for the criteria and the post-collision characteristics of three regimes. The transition criterion from coalescence to separation is given in terms of coalescence collision efficiency  $E_{coal}$  as follows (Brazier-Smith et al., 1972).

$$E_{coal} = \min \left[ 1, \frac{2.4f(\gamma)}{We_s} \right], \tag{4}$$

where,  $f(\gamma) = \gamma^3 - 2.4\gamma^2 + 2.7\gamma$ ,  $\gamma = D_2/D_1$  and  $We_s = \rho |\bar{u}_{rel}|^2 (D_1 + D_2) / 2\sigma$ . In addition, the subscripts

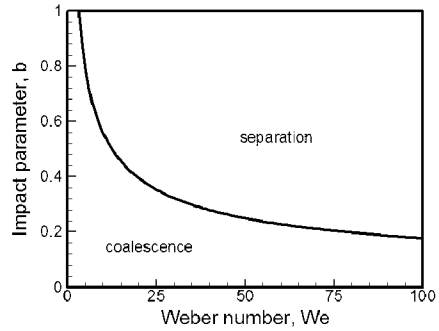


Fig. 3. Boundaries between collision regimes adopted in the O'Rourke model [1] model for  $\Delta=1$ .

1 and 2 represent smaller and larger droplets, respectively. The criterion of regime between coalescence and separation is determined by  $b = E_{coal}$ . In other words, coalescence occurs if impact parameter  $b$  is less than  $E_{coal}$  and otherwise the separation occurs.

The post-collision properties of the collision regimes such as droplet diameters and velocities are determined from the conservation equations of mass, linear momentum, and angular momentum (O'Rourke, 1981). In coalescence regime, the droplet mass and the velocity are expressed as

$$D_{1a} = \left( \frac{\rho_1 D_1^3 + n \rho_2 D_2^3}{\rho_{1a}} \right)^{1/3}, \tag{5}$$

$$\bar{u}_{1a} = \frac{(\rho_1 D_1^3 \bar{u}_1 + n \rho_2 D_2^3 \bar{u}_2)}{\rho_{1a} d_{1a}^3}, \tag{6}$$

where the subscript  $a$  denotes a value after collision and  $n$  is the number of coalescence. In the separation regimes, no mass is assumed to exchange between two colliding droplet parcels. The velocities are determined as

$$\bar{u}_{1a} = \frac{\rho_1 D_1^3 \bar{u}_1 + \rho_2 D_2^3 \bar{u}_2 + \rho_2 D_2^3 (\bar{u}_1 - \bar{u}_2) \left( \frac{b - \sqrt{E_{coal}}}{1 - \sqrt{E_{coal}}} \right)}{\rho_1 D_1^3 + \rho_2 D_2^3}, \tag{7}$$

$$\bar{u}_{2a} = \frac{\rho_1 D_1^3 \bar{u}_1 + \rho_2 D_2^3 \bar{u}_2 + \rho_2 D_2^3 (\bar{u}_2 - \bar{u}_1) \left( \frac{b - \sqrt{E_{coal}}}{1 - \sqrt{E_{coal}}} \right)}{\rho_1 D_1^3 + \rho_2 D_2^3}, \tag{8}$$

For more details, good summary is well documented in references (O'Rourke, 1981; Bai, 1996).

### 2.3 The present model

The present model is a modified version of the collision model, which is recently proposed by the authors (Ko and Ryou, 2005a, 2005b). Contrary to the O'Rourke model, the present model takes account for the stretching and reflexive separation regimes including the formation of satellite droplets. In addition, a criterion for bouncing regime is introduced and the dissipation energy during collision process is newly modeled to calculate the collision process of fuel droplets more accurately. Figure 4 shows the boundaries between the regimes adopted in the present model for the binary collision of equal-sized droplets.

In the present model, the criterion proposed by Estrade et al. (1999) is used to distinguish the bouncing collision from other regimes. When the following condition is satisfied, the bouncing occurs;

$$We < \frac{\Delta(1 + \Delta^2)(4\phi' - 12)}{\phi_2(\cos(\arcsin b))^2}, \tag{9}$$

where

$$\phi_2 = \begin{cases} 1 - (2 - \lambda)^2(1 + \lambda)/4 & \text{for } \lambda > 1.0 \\ \lambda^2(3 - \lambda)/4 & \text{for } \lambda < 1.0 \end{cases}$$

and  $\lambda = (1 - b)(1 + \Delta)$ . The shape factor  $\phi'$  is given a value of 3.351 by Estrade et al. (1999).

As seen in Fig. 5, the reflexive separation takes place for the head-on or near-centre collisions of two droplets, and the stretching separation occurs at the high impact parameter. Ashgriz and Poo (1990) explained two separation processes using the balance between the effective kinetic energy and the surface energy of the temporarily coalesced droplet. They proposed the boundaries from coalescence to reflexive and stretching separations as follows;

$$We > 3 \left[ 7(1 + \Delta^3)^{1/3} - 4(1 + \Delta^2) \right] \frac{\Delta(1 + \Delta^3)^2}{\Delta^6 \eta_1 + \eta_2} \tag{10}$$

(for reflexive separation),

$$We > \frac{4(1 + \Delta^3)^2 [3(1 + \Delta)(1 - b)(\Delta^3 \phi_1 + \phi_2)]^{1/2}}{\Delta^2 [(1 + \Delta^3) - (1 - b^2)(\phi_1 + \Delta^3 \phi_2)]} \tag{11}$$

(for stretching separation),

where the parameters  $\eta_1 = 2(1 - \xi)^2(1 - \xi^2)^{1/2} - 1$  and  $\eta_2 = 2(\Delta - \xi)^2(\Delta^2 - \xi^2)^{1/2} - \Delta^3$ , and  $\xi = (1/2)b(1 + \Delta)$ .

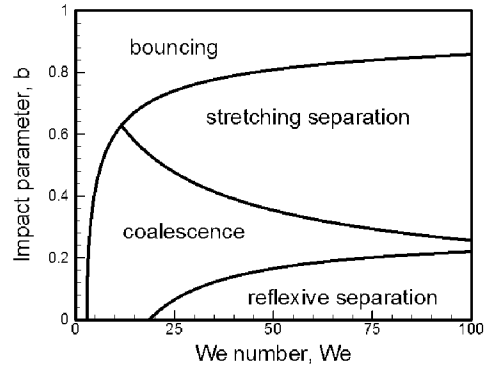


Fig. 4. Boundaries between collision regimes adopted in the new model for  $\Delta=1$ .

In addition,  $\phi_1$  and  $\phi_2$  denote the portions of interaction region (the hatched parts in Fig. 4(b)) of two colliding droplets for stretching separation, i.e.,

$$V_{1i} = \phi_1 V_1, \quad V_{2i} = \phi_2 V_2 \tag{12}$$

$$\phi_1 = \begin{cases} 1 - \frac{1}{4\Delta^3}(2\Delta - \lambda)^2(\Delta + \lambda) & \text{for } h > \frac{D_1}{2} \\ \frac{\lambda^2}{4\Delta^3}(3\Delta - \lambda) & \text{for } h < \frac{D_1}{2} \end{cases}, \tag{13}$$

$$\phi_2 = \begin{cases} 1 - \frac{1}{4}(2 - \lambda)^2(1 + \lambda) & \text{for } h > \frac{D_2}{2} \\ \frac{\lambda^2}{4}(3 - \lambda) & \text{for } h < \frac{D_2}{2} \end{cases}, \tag{14}$$

where  $\lambda \equiv (1 - b)(1 + \Delta)$  and the interaction height,  $h = 0.5(D_1 + D_2)(1 - b)$ .  $V$  is the volume of droplet,  $\Delta$  the size ratio of two droplets,  $b$  is the impact parameter, subscript  $i$  the interaction portion of droplets. Equations (10) and (11) showed good agreements with their experimental data (Ashgriz and Poo, 1990) for the regime boundaries between coalescence and separations. However, Ashgriz and Poo (1990) did not offer any empirical or theoretical relationship on the droplet velocities and sizes, which are essential for describing the separation processes numerically.

On the basis of Ashgriz and Poo (1990)'s theory, the present study newly derives the mathematical formulae for the post-collision characteristics in the reflexive and stretching separations. Both reflexive and stretching separation processes accompany with the formation of satellite droplet as shown in Fig. 5. In order to determine the volume separated from the colliding droplets, the present study introduces the new parameter  $C_V$ , called the separation volume

coefficient that is defined as the ratio of separating volume to interaction volume (the hatched parts in Fig. 4) between two colliding droplets. It is assumed that this coefficient  $C_V$  is proportional to the ratio of energy required for separation to total energy of two colliding droplets in the following manner.

$$C_V = \frac{KE_{sep} - SE_{coal}}{KE_{sep} + SE_{coal}}, \quad (15)$$

where  $KE_{sep}$  represents the effective kinetic energy inducing the separation of the temporarily combined droplets, and  $SE_{coal}$  is the effective surface tension energy retaining the coalescence between two droplets. The present study determines these effective energies for two different separation processes using the equations of Ashgriz and Poo (1990) as follows:

$$KE_{sep} = \begin{cases} \sigma \pi D_2^2 \left[ (1 + \Delta^2) - (1 + \Delta^3)^{2/3} + \frac{We(\Delta^6 \eta_1 + \eta_2)}{12\Delta(1 + \Delta^3)^2} \right] \\ \text{(for reflexive separation)} \\ \frac{1}{2} \rho u_{rel}^2 V_2^2 \left\{ \frac{\Delta^3 [(1 + \Delta^3) - (1 - b^2)(\phi_1 + \Delta^3 \phi_2)]}{(1 + \Delta^3)^2} \right\} \\ \text{(for stretching separation)} \end{cases} \quad (16)$$

$$SE_{coal} = \begin{cases} 0.75 \sigma \pi (D_1^3 + D_2^3)^{2/3} \\ \text{(for reflexive separation)} \\ \sigma [2\pi V_2 D_2 \lambda (\Delta^3 \phi_1 + \phi_2)]^{1/2} \\ \text{(for stretching separation)} \end{cases} \quad (17)$$

Using above equations, the separating volume and the size of colliding droplets after collision are calculated as follows:

$$V_s = C_v (V_{1t} + V_{2t}), \quad (18)$$

$$D_{ja} = (1 - C_v \phi_j)^{1/3} D_j, \quad (19)$$

where subscript  $a$  means a value after collision, and  $j = 1, 2$ .  $\phi$  is determined by Eqs. (13) and (14) for stretching separation, and is used the value of unity for reflexive separation because the interaction between two droplets occur over the whole volume of temporarily combined droplets [see Fig. 4 (a)].

For simplicity, all satellite droplets are assumed to have same properties. In turn, conservation equations for mass, momentum and energy are rewritten as

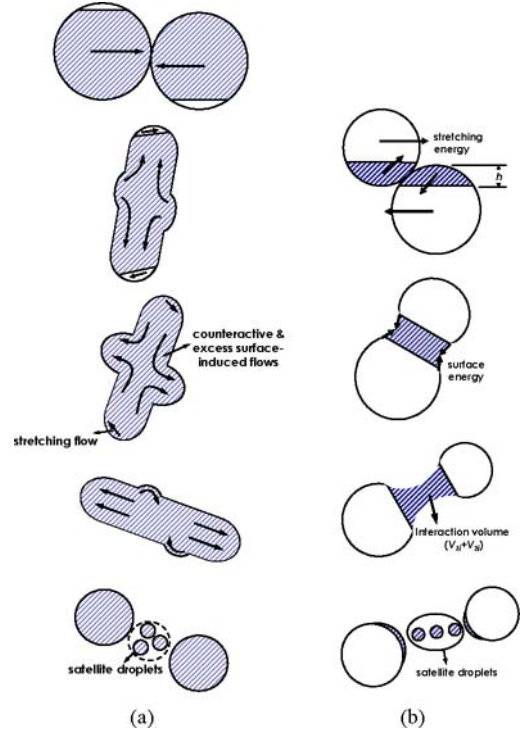


Fig. 5. Schematic of the (a) reflexive and (b) stretching separations after collision between two droplets.

$$\sum_{j=1}^2 D_j^3 = \sum_{j=1}^2 D_{ja}^3 + N_{sa} \cdot D_{sa}^3, \quad (20)$$

$$\sum_{j=1}^2 D_j^3 \vec{u}_j = \sum_{j=1}^2 D_{ja}^3 \vec{u}_{ja} + N_{sa} \cdot D_{sa}^3 \vec{u}_{sa}, \quad (21)$$

$$\begin{aligned} & \sum_{j=1}^2 \left( \frac{\pi}{12} \rho D_j^3 |\vec{u}_j|^2 + \sigma \pi D_j^2 \right) \\ &= \sum_{j=1}^2 \left( \frac{\pi}{12} \rho D_{ja}^3 |\vec{u}_{ja}|^2 + \sigma \pi D_{ja}^2 \right) \\ & \quad + KE_{sa} + SE_{sa} + EL \end{aligned} \quad (22)$$

where  $N$  is the number of droplets and subscript  $sa$  means the satellite droplet. Additionally,  $\vec{u}_1$  and  $\vec{u}_2$  are the velocities of the smaller and larger droplets in the mass-centre coordinates, respectively, as given by  $\vec{u}_1 = \vec{u}_{rel} / (1 + \Delta^3)$  and  $\vec{u}_2 = -\Delta^3 \vec{u}_{rel} / (1 + \Delta^3)$ , where  $\vec{u}_{rel}$  is the relative velocity of two droplets. The total kinetic energy of satellite droplets can be represented by

$$KE_{sa} = N_{sa} \cdot \left( \frac{\pi}{12} \rho D_{sa}^3 \right) |\vec{u}_{sa}|^2 = \frac{1}{2} \rho V_s |\vec{u}_{sa}|^2. \quad (23)$$

Also,  $EL$  denotes the energy loss consisting of

dissipation energy and surface tension energy loss as follow:

$$EL = \iint \mu \frac{1}{2} \left( \frac{\partial u_i}{\partial x_j} + \frac{\partial u_j}{\partial x_i} \right)^2 dV dt + \Delta S \sigma. \quad (24)$$

where  $\Delta S$  is the additional surface area associated with the deformation during collision process (Qian and Law, 1997)

In the our previous studies (Ko and Ryou, 2005a; 2005b), the following equation is derived on the basis of the relationship suggested by Jiang et al. (Jiang et al., 1992) who expressed the viscous dissipation in terms of the kinetic energy of interaction volume:

$$EL = \alpha \left( \frac{1}{2} \rho \sum_{j=1}^2 \phi_j V_j u_j^2 \right), \quad (25)$$

where  $\alpha$  denotes the energy loss coefficient. For water droplets,  $\alpha$  has been empirically determined to be around 0.5 by Jiang et al. (1992).

In this formula, the viscosity is excluded and the surface tension energy loss is also neglected. Qian and Law (1997), however, reported that the critical Weber number for the reflexive separation is dependent on the Ohnesorge number, representing the ratio of the viscous to surface energies. This means that the viscous dissipation and surface tension energy loss are significantly affected by the liquid properties in the reflexive separation regime. In this study, thus, a new formula is derived on the Qian and Law (1997)'s relationship for the energy loss during the reflexive separation process as follow:

$$EL = \frac{\pi D_1^2 \sigma}{24} \left\{ \frac{\alpha}{2} We + 16\sqrt{2}(1-\alpha)\beta Z + (1-\alpha)\gamma \right\} \quad (26)$$

where  $\beta$  and  $\gamma$  are the empirical constants and adopted as 30 and 15 from Qian and Law (1997), respectively, and  $Z = \mu / (\rho R \sigma)^{1/2}$  is the Ohnesorge number.

Considering the kinetic energy loss for the reflexive separation, the velocities of colliding droplets can be written as follows:

$$\vec{u}_{ja} = (1-\alpha)^{1/2} \vec{u}_j. \quad (27)$$

For the stretching separation, because the loss of kinetic energy is involved within the interaction portion which becomes the satellite droplets, the

colliding droplets can be assumed to retain their velocities, i.e.,

$$\vec{u}_{ja} = \vec{u}_j. \quad (28)$$

By solving the Eqs. (20) ~ (22) simultaneously, the characteristics of satellite droplets can be finally obtained as follows:

$$D_{sa} = \left[ \frac{C_v (\Delta^3 \phi_1 + \phi_2)}{N_{sa}} \right]^{1/3} D_2. \quad (29)$$

$$u_{sa} = \frac{\Delta^3 \phi_1 u_1 + \phi_2 u_2}{(\Delta^3 \phi_1 + \phi_2)}, \quad (30)$$

$$N_{sa} = \left[ \frac{SE_{sa}}{\sigma \pi C_v^{2/3} (\Delta^3 \phi_1 + \phi_2)^{2/3} D_2^2} \right]^3, \quad (31)$$

Now, the post-characteristics of the separation collisions can be calculated using Eqs. (19), and (27) ~ (31).

### 3. Results and discussion

This section examines the predictability of new model by comparing the predicted results with earlier published experimental data (Ashgriz and Poo, 1990; Qian and Law, 1997) for the binary collision of two droplets. Figure 6 shows the predicted *We-b* maps for the number of satellite droplets in case that the binary collision of two equal-sized water droplets takes place. In this calculation, the energy loss coefficient  $\alpha$  is 0.5 suggested by Jiang et al. (1992). In the stretching separation regime, the number of satellite droplets is of the highest value in the range from 0.4 to 0.6 in impact parameter. Until the impact parameter reaches to 0.4, the number of satellite droplets increases because of the increase in the stretching energy. When the impact parameter ranges from 0.6 to 1.0, on the other hand, the probability of satellite droplet formation is reduced due to the decrease in interaction region between two colliding droplets. In the reflexive separation regime, in addition, the satellite droplets are formed most actively in the case of the head-on collision. As mentioned previously, it can be supported by the fact that the stretching effects induced by off-centre collision reduce the reflexive separation. In Figs. 7 and 8, comparisons are made between the predictions and the experimental data of Ashgriz and Poo (1990) for the number of satellite

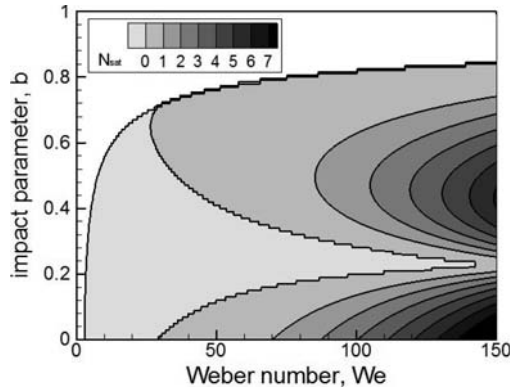


Fig. 6. Calculated number distribution of satellite droplets for binary collision of two water droplets for  $\Delta=1$ .

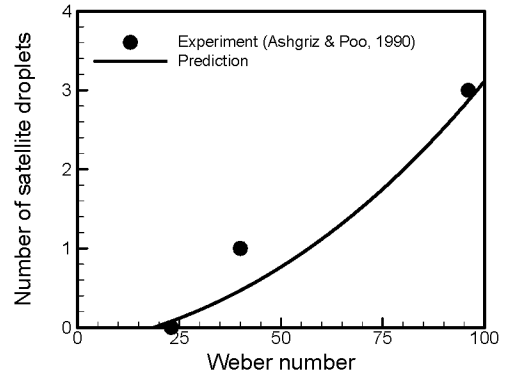


Fig. 8. Comparison of the calculated satellite droplets number with the experimental data (Ashgriz and Poo, 1990) for the head-on collision of two equal-sized water droplets.

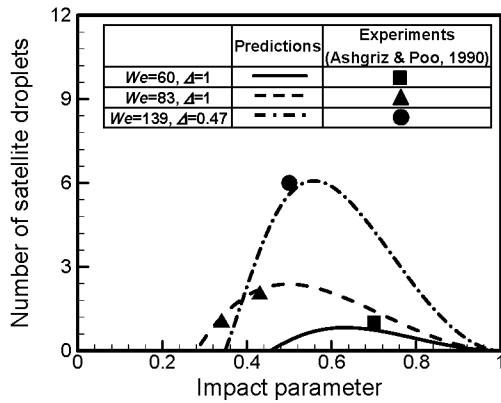


Fig. 7. Comparison of the calculated satellite droplet number with experimental data (Ashgriz and Poo, 1990) for stretching separation collision of two water droplets.

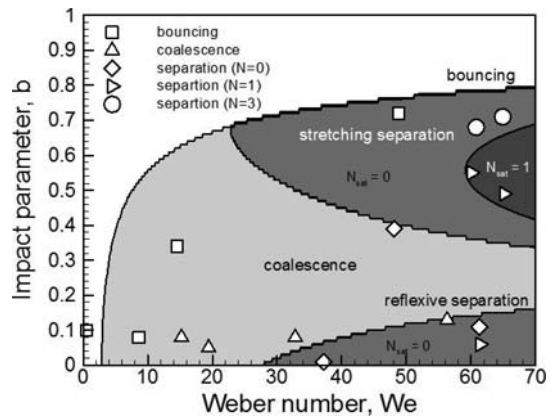


Fig. 9. Comparison of the calculated number distribution of satellite droplets with experimental data (Qian and Law, 1997) for the collision of equal-sized tetradecane droplets.

droplets. As seen in Figs. 7 and 8, the present model predicts well compared to the experimental data for the stretching separation and for the head-on collision at different conditions. For the head-on collision, it is found that the number of satellite droplets increase with the Weber number.

Figure 9 compares the predicted  $We$ - $b$  map for the collision of equal-sized tetradecane droplets with experimental data of Qian and Law (1997). Although some discrepancy between the predicted boundary of bouncing regime and experiments are shown at low Weber number, the predicted  $We$ - $b$  map represents well the overall distribution of collision regimes observed from experiment (1997).

In Fig. 10, the normalized mean diameter is presented for different Weber numbers and it is averaged over the whole range of impact parameter at a given Weber number. Here,  $D_{10}$  and SMD denote

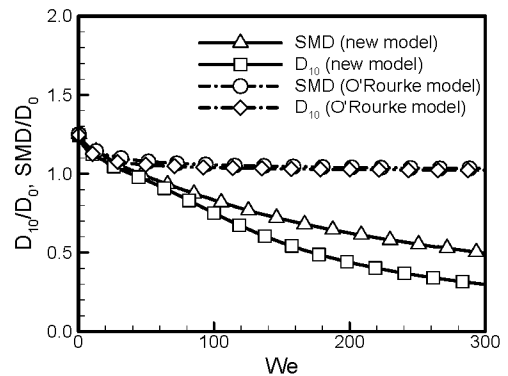


Fig. 10. Comparison between the predictions by both models for the  $D_{10}$  and SMD normalized by the initial droplet diameter  $D_0$  for the binary collision of equal-sized water droplets.

the arithmetic and Sauter mean diameters, respectively. They are often used to analyze the characteristics of droplet size distributions in applications of liquid spray. Over the range of low Weber number, both models predict the increase of mean diameter after collisions because of droplet coalescence. As the Weber number increases, however, both  $D_{10}$  and SMD computed by the new model decrease gradually, indicating that the droplet breakup via collision increases with Weber number. Since the O'Rourke model ignores the reflexive separation process at low impact parameters as well as the change in droplet size even in stretching separation process, the predictions of the O'Rourke model are rarely varied over the whole range of Weber number. From these results, it is concluded that the new model is more reasonable than the O'Rourke model for simulation in the droplet collision process leading to the droplet breakup.

#### 4. Conclusions

The present study has developed the binary droplet collision considering the collision-induced breakup and the effects of liquid property. In the present model, the post-collision characteristics of droplets were determined by the formulae based on the conservation equations between before and after collision. For the validation of the new model, the calculated results are first compared with experimental data (Ashgriz and Poo, 1990; Qian and Law, 1997) on the binary droplet collision. In the stretching separation regime, the number of satellite droplets is of the highest value in the range from 0.4 to 0.6 in impact parameter. In the reflexive separation regime, in addition, the satellite droplets are formed most actively in the case of the head-on collision. The predicted mean diameter by the new model decreased with increasing the Weber number because of the collision-induced breakup. The O'Rourke model, on the other hand, failed to predict the size reduction via the binary droplet collision. From these results, it can be concluded that the new model for droplet collision is more reasonable than the O'Rourke model for simulation in the collision-induced breakup process accompanied with formation of satellite droplets.

#### Acknowledgement

The authors would like to acknowledge the financial support from Ministry of Commerce, Industry and Energy (20055093).

#### References

- Arai, M., Saito, M., 1999, "Atomization Characteristics of Jet-to-Jet and Spray-to-Spray Impingement Systems," *Atomization and Sprays*, Vol. 9, pp. 399~417.
- Ashgriz, N., Poo, J. Y., 1990, "Coalescence and Separation in Binary Collisions of Liquid Drops," *Journal of Fluid Mechanics*, Vol. 221, pp. 183~204.
- Bai, C., 1996, *Modeling of Spray Impingement Processes*, Ph.D. thesis, Imperial College of Science and Technology and Medicine, Department of Mechanical Engineering, University of London.
- Brazier-Smith, P. R., Jennings, S. G., Latham, J., 1972, "The Interaction of Falling Water Droplets: Coalescence," *Proc. of the Royal Society of London A*, Vol. 326, pp. 393~408.
- Brenn, G., Valkovska, D., Danov, K. D., 2001, "The Formation of Satellite Droplets by Unstable Binary Drop Collisions," *Physics of Fluids*, Vol. 13, pp. 2463~2477.
- Estrade, J. P., Carentz, H., Lavergne, G. and Biscos, Y., 1999, "Experimental Investigation of Dynamic Binary Collision of Ethanol Droplets-a Model for Droplet Coalescence and Bouncing," *International Journal of Heat and Fluid Flow*, Vol. 20, pp. 486~491.
- Ko, G. H. and Ryou, H. S., 2005b, "Modeling of Droplet Collision-Induced Breakup Process," *International Journal of Multiphase Flow*, Vol. 31, pp. 723~738.
- Ko, G. H., Ryou, H. S., 2005a, "Droplet Collision Process in an Inter-Spray Impingement System," *Journal of Aerosol Science*, Vol. 36, pp. 1300~1321.
- O'Rourke, P. J., 1981, "Collective Drop Effects on Vaporizing Liquid Sprays," Ph.D. thesis, *Mechanical and Aerospace Engineering*, Princeton University, USA.
- Qian, J., Law, C. K., 1997, "Regimes of Coalescence and Separation in Droplet Collision," *Journal of Fluid Mechanics*, Vol. 331, pp. 59~80.